

Research Article

Unravelling the Complexity of Inherited Retinal Dystrophies Molecular Testing: Added Value of Targeted Next-Generation Sequencing

Isabella Bernardis,^{1,2} Laura Chiesi,³ Elena Tenedini,^{1,2} Lucia Artuso,^{1,2} Antonio Percesepe,⁴ Valentina Artusi,¹ Maria Luisa Simone,^{1,5} Rossella Manfredini,^{5,6} Monica Camparini,⁷ Chiara Rinaldi,⁷ Antonio Ciardella,⁸ Claudio Graziano,⁹ Nicole Balducci,⁸ Antonia Tranchina,⁹ Gian Maria Cavallini,³ Antonello Pietrangelo,^{1,2} Valeria Marigo,⁵ and Enrico Tagliafico^{1,2}

¹Center for Genome Research, University of Modena and Reggio Emilia, Modena, Italy

²Department of Medical and Surgical Sciences, University of Modena and Reggio Emilia, Modena, Italy

³Institute of Ophthalmology, University of Modena and Reggio Emilia, Modena, Italy

⁴Medical Genetics Unit, Azienda Ospedaliero-Universitaria di Parma, Parma, Italy

⁵Department of Life Sciences, University of Modena and Reggio Emilia, Modena, Italy

⁶Centre for Regenerative Medicine, University of Modena and Reggio Emilia, Modena, Italy

⁷Ophthalmology, S.Bi.Bi.T. Department, University of Parma, Parma, Italy

⁸Ophthalmology Unit, Policlinico S. Orsola-Malpighi, Bologna, Italy

⁹Medical Genetics Unit, Policlinico S. Orsola-Malpighi, Bologna, Italy

Correspondence should be addressed to Enrico Tagliafico; enrico.tagliafico@unimore.it

Received 15 June 2016; Revised 30 September 2016; Accepted 20 October 2016

Academic Editor: Ozgur Cogulu

Copyright © 2016 Isabella Bernardis et al. This is an open access article distributed under the Creative Commons Attribution License, which permits unrestricted use, distribution, and reproduction in any medium, provided the original work is properly cited.

To assess the clinical utility of targeted Next-Generation Sequencing (NGS) for the diagnosis of Inherited Retinal Dystrophies (IRDs), a total of 109 subjects were enrolled in the study, including 88 IRD affected probands and 21 healthy relatives. Clinical diagnoses included Retinitis Pigmentosa (RP), Leber Congenital Amaurosis (LCA), Stargardt Disease (STGD), Best Macular Dystrophy (BMD), Usher Syndrome (USH), and other IRDs with undefined clinical diagnosis. Participants underwent a complete ophthalmologic examination followed by genetic counseling. A custom AmpliSeq™ panel of 72 IRD-related genes was designed for the analysis and tested using Ion semiconductor Next-Generation Sequencing (NGS). Potential disease-causing mutations were identified in 59.1% of probands, comprising mutations in 16 genes. The highest diagnostic yields were achieved for BMD, LCA, USH, and STGD patients, whereas RP confirmed its high genetic heterogeneity. Causative mutations were identified in 17.6% of probands with undefined diagnosis. Revision of the initial diagnosis was performed for 9.6% of genetically diagnosed patients. This study demonstrates that NGS represents a comprehensive cost-effective approach for IRDs molecular diagnosis. The identification of the genetic alterations underlying the phenotype enabled the clinicians to achieve a more accurate diagnosis. The results emphasize the importance of molecular diagnosis coupled with clinic information to unravel the extensive phenotypic heterogeneity of these diseases.

1. Introduction

Inherited Retinal Dystrophies (IRDs) are a heterogeneous group of eye disorders characterized by rod and/or cone

photoreceptor cells degeneration, which include Retinitis Pigmentosa (RP), Leber Congenital Amaurosis (LCA), Stargardt Disease (STGD), Best Macular Dystrophy (BMD), and syndromic forms such as Usher Syndrome (USH).

TABLE 1: Patients cohort.

Clinical diagnosis	Number of cases	Healthy relatives	Familiar Cases (number of families)	Presumed inheritance in family				Sex		Age at genetic counseling	
				Sporadic	AD	AR	XL	M	F	Range	Median
BMD	4		2 (1)		4			1	3	12–65	58
LCA	5	5		1		4		2	3	5–85	9
STGD	14		6 (3)			14		5	9	8–59	28
RP	45	12	9 (4)	14	6	20	5	25	20	2–73	47.5
USH	3					3		2	1	33–53	51
nd IRD	17	4	6 (2)	6	6	5		13	4	2–62	35
Total	88	21	23 (10)	21	16	46	5	48	40	2–85	37

BMD: Best Macular Dystrophy; LCA: Leber Congenital Amaurosis; STGD: Stargardt disease; RP: Retinitis Pigmentosa; USH: Usher syndrome; nd IRD: inherited retinal degeneration not otherwise specified without precisely defined diagnosis; AD: autosomal dominant; AR: autosomal recessive; XL: X-linked; M: male; F: female.

The overall prevalence of these disorders is ~1 in 4,000 individuals for RP, ~1 in 90,000 individuals for LCA and USH, ~1 in 5,000–10,000 individuals for STGD, and 1/5000–1/67000 for BMD (<http://www.orpha.net>). Classification of IRDs considers the principal site of retinal dysfunction (rod, cone, retinal pigment epithelium, or inner retina), the mode of inheritance, the underlying gene defect, typical age of onset, rate of progression, and association with systemic syndromes. The genetic bases of IRDs are highly heterogeneous, with almost 150 genes currently known [RetNet, <https://sph.uth.edu/retnet/>] and a wide clinical and genetic overlap among the different disorders, with high phenotypic variability and genes associated with more than one phenotype. The inheritance of these diseases is also complex, with autosomal dominant (AD), autosomal recessive (AR), X-linked (XL), and even digenic patterns [1]. The extensive clinical and genetic heterogeneity in IRD, along with the variable age of onset, the incomplete penetrance, and unclear inheritance, hamper clinical diagnosis.

Recently, Next-Generation Sequencing (NGS) has been used for the genetic diagnosis of retinal diseases [2–6] and has been reported as a cost-effective approach [7, 8] with a wide range of reported mutation detection rates related to differences in number of genes analyzed, NGS platform, and cohort size but above all composition of the study case phenotypes. We therefore present a multidisciplinary approach coupled with a comprehensive NGS amplicon-based strategy to explore IRD genetic complexity and evaluate genotype-phenotype correlations.

2. Patients and Methods

This study was approved by the ethics committee (Comitato Etico di Modena, Modena, Italy). The procedures followed were in accordance with the Helsinki Declaration of 1975, as revised in 2000, and samples were obtained after patients had provided written informed consent.

A total of 109 samples were collected, including 88 IRDs affected probands with unknown molecular diagnosis and 21 healthy family members (Table 1). Subjects were recruited at the Medical Genetics Unit of the University Hospital of

Modena (70 samples), at the Medical Genetics Unit of Parma University Hospital (15 samples) and Medical Genetics Unit of Policlinico Sant'Orsola Malpighi, Bologna (24 samples). All subjects underwent a complete ophthalmologic examination (visual acuity, anterior segment and fundus examination, spectral domain-optical coherence tomography, electroretinogram, and/or electrooculogram) followed by genetic counseling. When indicated fundus autofluorescence imaging and visual field were also performed. Clinical information for the patients with identified pathogenic mutations is shown in Supplementary Table 1 (in Supplementary Material available online at <http://dx.doi.org/10.1155/2016/6341870>). Clinical diagnoses of participating subjects included RP, USH (hearing impairment + RP), LCA, STGD, BMD, and IRDs not otherwise specified or with imprecisely defined clinical diagnosis. Four control patients with known molecular diagnosis were used to validate our method.

2.1. AmpliSeq Panel Design and Ion Torrent™ PGM™ Library Preparation and Sequencing. The Ion AmpliSeq technology (Life Technologies Ltd., Paisley, UK) was used to design a panel of 72 genes (Supplementary Table 2) associated with the following IRD forms: RP, LCA, STGD, BMD, and USH [RetNet, <https://sph.uth.edu/retnet/>]. The Ion AmpliSeq Designer tool (<https://www.ampliseq.com/browse.action>) generated an optimized primers design encompassing the coding DNA sequence of the selected genes, for a total of 1.649 amplicons divided into two pools to optimize coverage and multiplex PCR conditions. Libraries were prepared using the Ion AmpliSeq Library Kit 2.0 starting from 15 ng of gDNA/pool according to manufacturer's recommendations. Template preparation was performed using an Ion OneTouch™ 2 System following the latest version of the manufacturer's manuals. The template positive Ion Sphere Particles (ISPs+) were sequenced on an Ion Torrent Personal Genome Machine® (PGM) System (Life Technologies Ltd., Paisley, UK) using the Ion 318™ Chip kit v2 following the Ion PGM Sequencing 200 Kit v2 manual.

2.2. Sanger Sequencing. Sanger sequencing was performed to validate *CNGBI* c.875-5.891dup mutation (identified with

an anomalous distribution of NGS reads attributable to amplification problems due to the insertion itself located at the end of the target region) and to sequence *RPGR* ORF15 partially uncovered by the NGS panel. Primers for PCR and sequencing are shown in Supplementary Table 3. The following conditions were used: a 50 μ L PCR reaction containing 100 ng of DNA, 100 pmol of forward and reverse primers, 5 μ L of buffer, and 0.5 μ L of Taq Expand High Fidelity™ DNA Polymerase (Roche). PCR amplification (see Supplementary Table 3) was performed using a Gene Amp PCR System 9700 (Applied Biosystems, California, USA). The resultant amplicons were purified using High Pure PCR Product Purification Kit (Roche). Additional primers for *RPGR* sequencing were used. The sequencing reactions were performed with BigDye Terminator v1.0 (Life Technologies) and run on ABI PRISM® 3130XL Genetic Analyzer (Life Technologies). Due to sequence composition and technical difficulties, part of *RPGR* ORF15 (~250 bp, chrX: 38145343–38145593) could not be accurately sequenced with Sanger sequencing.

2.3. Data Analysis. Samples were processed using the Ion Torrent Suite™ (TS) Software for raw data processing and sequence alignment to the human genome reference sequence hg19. The TS Variant Caller was used for the detection of germline variants that were subsequently analyzed using the following optimized filtering and annotation pipeline. Annovar [9] and Variant Effect Predictor (VEP) [10] were used to functionally annotate the detected variants, retrieving RefSeq gene annotation, dbSNP rs identifiers, ClinVar accession, and allele frequency observed in the population (1000-Genome Project, NHLBI GO Exome Sequencing Project ESP6500SI-V2, Exome and Aggregation Consortium ExAC 0.3). Variants with low coverage or low frequency (<30 reads or <30%, resp.) were filtered out. The synonymous variants and variants having an allele frequency greater than 1% reported in the population were discarded as well. In addition, an internal database, built with all variants present in our cohort of processed samples, allowed recognizing and classifying as polymorphisms variants not listed in public databases. Variants were further annotated with conservation scores and functional predictions listed in dbNSFP [11–13], a database which compiles scores from various prediction algorithms, among which are SIFT, Polyphen2, LRT, MutationTaster, MutationAssessor, and FATHMM. Retina International (<http://www.retina-international.org/>), *RPGR* database (http://rpgr.hgu.mrc.ac.uk/index.php?select_db=RPGR), CEP290base (<http://cep290base.cmgg.be/>), and BEST1 LOVD database (http://www.huge.uni-regensburg.de/BEST1_database) were used to explore additional annotations and literature information, if present. Splice-altering predictions were obtained using the online tools Human Splicing Finder (HSF 3.0) [14] and NNSPLICE 0.9 [15] and the databases dbSCSNV [16] and SPIDEX [17], which provide predicted effects for all of the potential variants within splicing consensus regions or across the entire genome, respectively. For the prioritization of pathogenetic mutations, the evaluation of inheritance mode was taken into account, along with segregation information

coming from the sequencing of healthy family members, if available.

NGS procedure and data analysis were tested on the four control samples with known molecular diagnosis as proof of concept. In all cases the previously identified variants were correctly detected and prioritized as pathogenic variants.

3. Results

A cohort of 109 samples (Table 1), including 88 IRDs affected probands without molecular diagnosis and 21 unaffected family members, was analyzed by the newly developed system based on NGS and data analysis. A total of 19 sequencing runs were performed (6 samples/Ion Chip 318), obtaining on average a mean coverage of 450 mapped reads, with 92% mean uniformity and 97.6% (SD \pm 1.4) of target regions covered at least 30x (96.2% > 50x). For each sample, 242 raw variants were detected on average. Annotation and filtering procedure resulted in the identification of possibly causative mutations in 59.1% of patients ($n = 52/88$) (Table 2, Figure 1). The majority of the obtained molecular diagnoses were consistent with the subject's clinical presentation and family history.

We found pathogenic mutations in 16 genes, with the most recurrent being *ABCA4* for STGD and *USH2A* for RP/USH patients. The majority of the mutated genes were inherited with an AR pattern (78.9%), followed in order by AD (11.5%) and XL (9.6%) inheritance. The majority of cases displaying recessive inheritance were compound heterozygous of two different pathogenic variants, in line with the low frequency of consanguineous marriages in Italy

Identified candidate pathogenic mutations are shown in Table 3. Overall, 63 different mutations were identified: 62.5% of variants were already reported in previous studies, while 37.5% were novel. Among the list of novel variants, 56% were missense predicted to have deleterious protein functional effect by the prediction algorithms described in the Patients and Methods (predicted to be damaging by at least three of the applied algorithms), and 44% were frameshift, nonsense, or splice-site mutations that might severely affect protein function. Notably, 12% of identified variants were located within splicing consensus regions, and additional 12% were exonic variants predicted to alter splicing through enhancer/silencer motif modification or the creation of new potential donor/acceptor sites.

Table 2 summarizes the mutation detection rates obtained for the different clinical subtypes of our study cohort. The highest diagnostic yields were achieved for BMD, LCA, USH, and STGD patients with well-defined clinical diagnosis, where the number of known genes associated with each disease is relatively limited.

For BMD cases, all diagnosed patients were heterozygous for mutations on *BEST1*. Three patients (mother and son) were found to harbour a novel *BEST1* missense mutation c.80G>C (p.Ser27Thr) located in the immediate N-terminus, in one of the four mutational hotspots regions in the highly conserved N-terminal half of the protein [18] and predicted to be deleterious by all interrogated algorithms.



FIGURE 1: The chart summarizes the diagnostic yields obtained for the clinical subtypes of this study. The different levels of circles (from inner to outside) specify clinical diagnoses, inheritance mode, mutated genes, and clinical reassessment.

TABLE 2: Diagnostic yields for the clinical subtypes of this study.

Clinical diagnosis	Cases (n)	Genetic diagnosis (n)	Unsolved cases (n)	Clinical reassessment (final diagnosis)	Diagnostic yield (%)
BMD	4	4	—		100
LCA	5	4	1		80
STGD	14	11	3		78.5
RP	45	27	18	2 (USH)	60.0
USH	3	3	—		100
nd IRD	17	3	14	3 (ACHM, LCA, STGD)	17.6
Total	88	52	36	5	59.1

BMD: Best Macular Dystrophy; LCA: Leber Congenital Amaurosis; STGD: Stargardt Disease; RP: Retinitis Pigmentosa; USH: Usher Syndrome; nd IRD: inherited retinal degeneration not otherwise specified without precisely defined diagnosis; ACHM: Achromatopsia.

TABLE 3

Patient ID	Family	Clinical diagnosis	Clinical reassessment	Genotype	Inheritance	Gene	Mutation type	Region	cds change
IRD027		STGD		Comp Het	ar	ABCA4	Splice_region	INTRON_40	c.5714+5G>A
IRD036		STGD		Comp Het	ar	ABCA4	Frameshift	EXON_11	c.1375delA
IRD037	Familial case	STGD		Comp Het	ar	ABCA4	Stop_gained	EXON_14	c.2099G>A
IRD042		STGD		Comp Het	ar	ABCA4	Splice_region syn	EXON_6	c.768G>T
IRD043	Familial case	STGD		Comp Het	ar	ABCA4	Stop_gained	EXON_14	c.2099G>A
IRD050		STGD		Comp Het	ar	ABCA4	Splice_region syn	EXON_6	c.768G>T
IRD054		STGD		Comp Het	ar	ABCA4	Missense	EXON_42	c.5882G>A
IRD055		STGD		Comp Het	ar	ABCA4	Missense	EXON_6	c.634C>T
IRD061		STGD		Comp Het	ar	ABCA4	Missense	EXON_42	c.5882G>A
IRD062		STGD		Comp Het	ar	ABCA4	Missense	EXON_42	c.5882G>A
IRD073		nd IRD	STGD	Hom	ar	ABCA4	Missense	EXON_12	c.1622T>C
IRD077		STGD		Comp Het	ar	ABCA4	Missense	EXON_16	c.2461T>A
IRD047		BMD		Het	ad	BEST1	Stop_gained	EXON_15	c.2300T>A
IRD057	Familial case	BMD		Het	ad	BEST1	Missense	EXON_47	c.6445C>T
IRD058		BMD		Het	ad	BEST1	Missense	EXON_42	c.5882G>A
IRD064		BMD		Het	ad	BEST1	Missense	EXON_42	c.5882G>A
IRD010		LCA		Comp Het	ar	CEP290	Missense	EXON_19	c.2894A>G
IRD066		RP		Comp Het	ar	CEP290	Missense	EXON_37	c.5285C>A
						CEP290	Frameshift	EXON_15	c.2300T>A
						CEP290	Stop_gained	EXON_2	c.73C>T
						CEP290	Frameshift	EXON_2	c.80G>C
						CEP290	Stop_gained	EXON_2	c.80G>C
						CEP290	Frameshift	EXON_2	c.80G>C
						CEP290	Stop_gained	EXON_2	c.80G>C
						CEP290	Frameshift	EXON_2	c.80G>C
						CEP290	Stop_gained	EXON_33	c.4237G>C
						CEP290	Frameshift	EXON_23	c.2390delA
						CEP290	Stop_gained	EXON_48	c.6640A>T
						CEP290	Frameshift	EXON_14	c.1219_1220delAT

TABLE 3: Continued.

IRD072	nd IRD	LCA	Comp Het	ar	CEP290	Missense	EXON_14	c.1298A>G
IRD039	RP		Hom	ar	CEP290	Frameshift	EXON_3	c.164_167delCTCA
IRD052	RP		Comp Het	ar	CNGBI	Frameshift	EXON_13	c.875-5_891dup
IRD068	RP		Comp Het	ar	CNGBI	Missense	EXON_29	c.2957A>T
IRD085	RP		Comp Het	ar	CNGBI	Frameshift	EXON_13	c.875-5_891dup
IRD032	nd IRD	ACHM	Comp Het	ar	CNGBI	Splicing, syn	EXON_26	c.2526C>T
IRD029	RP		Hom	ar	CNGBI	Missense	EXON_21	c.2153G>C
IRD030	RP		Hom	ar	CNGBI	Missense	EXON_23	c.2284C>T
IRD031	RP		Hom	ar	CNGBI	Missense	EXON_23	c.2284C>T
IRD035	LCA		Het	ad	CRX	Frameshift	EXON_4	c.514delC
IRD008	RP		Hom	ar	PDE6B	Splice_region	EXON_18	c.2193+1delG
IRD013	RP		Comp Het	ar	PDE6B	Missense	EXON_4	c.794G>A
IRD026	RP		Het	ad	PDE6B	Intron	INTRON_8	c.1108-10G>A
IRD016	RP		Comp Het	ar	RHO	Missense	EXON_3	c.568G>T
IRD033	RP		Hem	xl	ROMI	Missense	EXON_1	c.178C>A
IRD076	RP		Hom	ar	ROMI	Missense	EXON_1	c.323C>T
IRD001	RP		Comp Het	ar	RP2	Frameshift	EXON_2	c.382_383delTT
IRD074	LCA		Hom	ar	RPE65	Missense	EXON_2	c.65T>C
IRD002	LCA		Comp Het	ar	RPE65	Missense	EXON_2	c.65T>C
IRD012	RP		Hem	xl	RPE65	Frameshift	EXON_9	c.893delA
IRD067	RP		Hem	xl	RPE65	Missense	EXON_5	c.430T>G
IRD075	RP		Hem	xl	RPE65	Missense	EXON_5	c.2225_2226delGA
IRD017	RP		Hem	De novo	RPGRIP1	Frameshift	EXON_15	c.2795_2796insT
IRD059	RP		Comp Het	ar	RPGRIP1	Frameshift	EXON_17	c.785C>G
IRD060	RP		Comp Het	ar	RPGR	Missense	EXON_8	c.814G>T
IRD041	RP		Comp Het	ar	RPGR	Missense, Splice_region	EXON_8	c.814G>T
					RPGR	Splice_region	EXON_2	c.154G>A
					RPGR	Frameshift	EXON_2	c.89delT
					TULPI	Missense	EXON_15	c.1590C>G
					TULPI	Missense	EXON_13	c.1255C>T
					TULPI	Missense	EXON_15	c.1590C>G
					TULPI	Missense	EXON_15	c.1590C>G
					TULPI	Splice_region	INTRON_14	c.1496-6C>A
					TULPI	Missense	EXON_13	c.1255C>T
					TULPI	Missense	EXON_14	c.1445G>A

TABLE 3: Continued.

IRD007	USH	Comp Het	ar	USH2A	Missense	EXON_63	c.12420T>G
IRD009	USH	Comp Het	ar	USH2A	splice_region, syn	EXON_28	c.5775A>T
IRD021	RP	Comp Het	ar	USH2A	splice_region, Missense	EXON_63	c.13546G>T
IRD023	RP	Comp Het	ar	USH2A	Missense	EXON_10	c.1645T>C
IRD024	RP	Comp Het	ar	USH2A	Missense	EXON_69	c.14995A>G
IRD038	RP	Comp Het	ar	USH2A	Missense	EXON_8	c.1481A>G
IRD084	USH	Hom	ar	USH2A	Frameshift	EXON_13	c.2296T>C
IRD034	RP	Hom	ar	USH2A	Frameshift	EXON_3	c.545_548delAAGA
				USH2A	Missense	EXON_13	c.2296T>C
				USH2A	Missense	EXON_13	c.2296T>C
				USH2A	Frameshift	EXON_69	c.14977_14978delTT
				USH2A	Missense	EXON_63	c.12574C>T

TABLE 3: Continued.

Patient ID	Protein change	Frequency (%)	Coverage (# reads)	Segregation and unaffected siblings	Functional predictions (dbNSFP)	Human Splicing Finder	Splicing predictions		Reference
							dbscSNV	SPIDEX	
IRD027		44.9	514			Broken WT Donor Site	0.999 0.988	-3.21	PMID: 15494742
IRD036	p.Thr459GlnfsX2	47.7	1179			Broken WT Donor Site	1.000 0.952	-2.43	PMID: 21911583
	p.Trp700X	48.2	303		. .N AD				PMID: 11702214
IRD037	p.Val256Val	47.2	53			New Acceptor Site	1.000 0.952	-5.41	PMID: 12037008
	p.Trp700X	44.5	110		. .N AD				PMID: 11702214
IRD042	p.Val256Val	48.3	29			Broken WT Donor Site	1.000 0.952	-2.43	PMID: 12037008
	p.Gly1961Glu	47.1	1325		D D D D N D D D D D				PMID: 9295268
IRD043	p.Arg212Cys	49.1	432			Broken WT Donor Site	1.000 0.952	-2.43	PMID: 11726554
	p.Gly1961Glu	46.9	796		D D D D A M D D D D D				PMID: 9295268
IRD050	p.Leu541Pro	51.9	727			Broken WT Donor Site	1.000 0.952	-2.43	PMID: 9295268
	p.Trp821Arg	43.8	309		D D D D A M D D D D D				PMID: 11527935
IRD054	p.Val767Asp	46.3	452			New ESS site	1.000 0.952	-58.3	PMID: 11527935
	p.Arg2149X	49.1	422		D D D D H T D D D D D				PMID: 15494742
IRD055	p.Gly1961Glu	49.4	1448			New ESS site	1.000 0.952	-58.3	PMID: 12202497
	p.Arg948Cys	52.0	175		. .D AD				PMID: 9295268
IRD061	p.Val767Asp	51.5	437			New ESS site	1.000 0.952	-58.3	This study
	p.Gly1961Glu	50.0	729		D D D D N D D D D D				PMID: 15494742
IRD062	p.Pro1380Leu	55.8	437			New ESS site	1.000 0.952	-58.3	PMID: 9295268
	p.Gly1961Glu	100	787		D D D D N D D D D D				PMID: 11726554
IRD073	p.Tyr850Cys	49.4	176			New ESS site	1.000 0.952	-58.3	PMID: 9295268
	p.Asn965Ser	100	225		D D D D M T D D D D D				PMID: 23096905
IRD077	p.Alal762Asp	50.8	259			New Donor Site, New ESS site	1.000 0.952	-58.3	PMID: 9054934
	p.Val767Asp	51.4	752		D D D D A M D D D D D				PMID: 15192030
IRD047	p.Arg25Trp	56.0	348			New Donor Site, New ESS site	1.000 0.952	-58.3	PMID: 15494742
IRD057	p.Ser27Thr	46.8	344			New Donor Site, New ESS site	1.000 0.952	-58.3	PMID: 10798642
IRD058	p.Ser27Thr	45.5	317		D D D U D H D D D D D				This study
IRD064	p.Ser27Thr	47.1	453			New Donor Site, New ESS site	1.000 0.952	-58.3	This study
	p.Aspl413His	49.2	413		D D D U D H D D D D D				This study
IRD010	p.Lys797SerfsX2	30.1	163			New Donor Site, New ESS site	1.000 0.952	-58.3	This study
	p.Lys2214X	47.5	705		D D D U D H D D D D D				ClinVar: RCV000082249.5
IRD066	p.Met407GlnfsX14	51.1	225			New Donor Site, New ESS site	1.000 0.952	-58.3	This study
					. .D AD				PMID: 17724218

TABLE 3: Continued.

IRD	Mutation	Age	Sex	Family	Genotype	Phenotype	ESS site	Study
IRD072	p.Asp433Gly	53.4	116		T D P D D L L T T T D D	New ESS site, New donor site	This study	
IRD039	p.Thr55SerfsX3	43.2	243				PMID: 20690115	
IRD052	p.Gly298CysfsX13	100*	471		D D D D D M D D D D D D		This study	
	p.Asn986Ile	51.7	258				PMID: 21147909	
	p.Gly298CysfsX13	26, 7*	431			ESE Site Broken	This study	
IRD068	Thr842Thr	52.1	153		D P P D D M T T T D D		This study	
	p.Gly718Ala	47.1	57		D D D D D H D D D D D D		This study	
IRD085	p.Arg762Cys	100	907			Broken WT Donor Site	This study	
IRD032		47.8	588				PMID: 15657609	
	p.Thr383IlefsX13	46.5	397		D D D D D M T D D D D D		PMID: 15657609	
IRD029	p.Gly734Arg	100	397		D D D D D M T D D D D D		This study	
IRD030	p.Gly734Arg	100	397		D D D D D M T D D D D D		This study	
IRD031	p.Gly734Arg	100	397		D D D D D M T D D D D D		This study	
IRD035	p.Pro172LeufsX15	50.5	521				This study	
IRD008		100	395	Brother: Het		Broken WT Donor Site	This study	
IRD013	p.Arg265Gln	51.7	319	n.a.	T D D D D L L T T T N D		ClinVar: RCV000178068.1	
		54.7	75	Mother: Het		0.001 0.096	PMID: 8698075	
IRD026	p.Asp190Tyr	44.6	168		D D D D D M T T T D D D		PMID: 8401533	
IRD016	p.Pro60Thr	56.1	278		T B B N N L T T T N N		PMID: 8595413	
	p.Thr108Met	52.8	108		T P B N D L T T T N D		PMID: 8595413	
IRD033	p.Leu129ValfsX9	100	392				This study	
IRD076	p.Leu22Pro	100	495		T B B D D M D D D N D		PMID: 9801879	
IRD001	p.Leu22Pro	46.3	257	Brother: wt	T B B D D M D D D N D		PMID: 9801879	
	p.Lys298SerfsX27	98	150	Brother: wt			PMID: 11462243	
IRD074	p.Tyr144Asp	100	430	Father: Het	D D D D D M D D D D D		PMID: 11462243	
IRD002	p.Glu743ArgfsX24	48.8	570	Father: Het			This study	
	p.Glu933X	48.8	400	Mother: Het			This study	
IRD012	p.Ala262Gly	100	280		T B B N N L D T T N N		This study	
IRD067	p.Gly272Cys	100	155		D D D D D H D D D D D		This study	
IRD075	p.Gly52Arg	100	348		D D P U D M T T T D D	Broken WT Donor Site	PMID: 15364249	
IRD017	p.Phe30SerfsX38	100	113	Brother: wt Female twin: wt			This study	
IRD059	p.Ile530Met	50.6	682		D D D D D H D D D D D N		This study	
	p.Arg419Trp	49.5	645		D D D D D H D D D D D D		PMID: 25342620	
IRD060	p.Ile530Met	51.0	655		D D D D D H D D D D D N		This study	
	p.Arg419Trp	45.3	575		D D D D D H D D D D D D		PMID: 25342620	
IRD041		54.1	727	Father: Het		0.005 0.419	PMID: 9660588	
	p.Arg482Gln	48.5	485	Mother: Het	D D D D D H D D D D D D		PMID: 22665969	

TABLE 3: Continued.

IRD007	p.Cys4140Trp	50.5	214	D D D D D M T T T D D	Broken WT Donor Site	0.998 0.986	-4.24	This study
IRD009	p.Gly4516Trp	49.5	398	D D U D H T D D D D		0.417 0.520		This study
	p.Cys549Arg	53.8	239	D D U D H D D D D D				This study
	p.Thr4999Ala	49.2	566	D D U D H D D D D D				This study
IRD021	p.Thr4999Ala	51.0	400	D D U D M T T T D D				This study
	p.Tyr494Cys	49.0	400	D D N D L T T T D D				This study
IRD023	p.Cys766Arg	39.0	82	D D D D D H D D D D D				PMID: 23591405
	p.Lys182ArgfsX9	61.4	202	D D D D H D D D D D D				This study
IRD024	p.Cys766Arg	43.5	124	D D D D H D D D D D D				PMID: 23591405
	p.Lys182ArgfsX9	48.0	225	D D D D H D D D D D D				This study
IRD038	p.Cys766Arg	47.2	89	D D D D H D D D D D D				PMID: 23591405
	p.Cys759Phe	51.1	90	D D D A H D D D D D D				PMID: 10775529
IRD084	p.Phe4993ProfsX7	100	483					PMID: 24944099
IRD034	p.Arg4192Cys	100	515	D D P N D M D D D D D				PMID: 24498627

ACHM: Achromatopsia; ad: autosomal dominant; ar: autosomal recessive; BMD: best macular disease; Comp Het: compound heterozygous; ESE: exonic splicing enhancer; ESS: exonic splicing silencer; Hem: Hemizygous; Het: heterozygous; Hom: homozygous; LCA: Leber Congenital Amaurosis; nd IRD: inherited retinal degeneration not otherwise specified without precisely defined diagnosis; RP: Retinitis Pigmentosa; STGD: Stargardt Disease; USH: Usher Syndrome; wt: wild-type; xl: X-linked. For nonsynonymous variants, predictions from dbNSFP are reported, comprising scores from the following algorithms: SIFT | Polyphen2HDIV Polypehn2HVAR | LRT | MutationTaster | MutationAssessor | FATHMM | MetaSVM | MetaLR | PROVEAN | fathmm-MKL. For splicing variants, predictions from Human Splicing Finder, dbSnp (ada.score|rf.score) and SPIDEX are reported. For SPIDEX, max dPSI is shown if lower than -1 (maximum mutation - induced change in the percentage of transcripts with the exon spliced in). Familiar case: the patients were from the same family. * Sanger sequencing was performed to confirm mutation frequency.

For STGD patients, genetic diagnosis was achieved in 11 out of 14 (78.5% of the cases). All diagnosed patients in our cohort carried mutations on *ABCA4*. In 75% of the unsolved cases at least one *ABCA4* pathogenic allele was identified, suggesting the presence of disease-causing mutations lying outside the coding sequence covered by our panel, as reported in a previous study [19].

In LCA patients, causative mutations were identified in *CEP290*, *RPE65*, *RPGRIP1*, and *CRX* genes, and only one case remained unsolved (20% of the total LCA cases), whereas all Usher 2 syndrome cases were found to carry mutations in *USH2A* gene.

For RP patients, genetic diagnosis was achieved in 27 out of 45 (60% of the cases), involving mutations in 11 different genes: confirming that these phenotypes are genetically heterogeneous (Figure 1). Dominant mutations were identified in *RHO* gene, whereas *USH2A*, *CNGBI*, and *TULP1* were the most recurrently mutated genes in ARRP. X-linked inheritance was established for 5 RP male patients (4 probands had mutations in *RPGR*, whereas one had a mutation in *RP2*). The identification of *USH2A* as the defective gene in patients with initial clinical diagnosis of RP was followed by audiometric testing to establish if there were any hearing deficiencies. A hearing impairment was found in 2 cases out of 5 leading to clinical reassessment and final diagnosis of USH (Table 2).

For patients with IRD without a defined clinical diagnosis or with unclear disease manifestations, we identified causative mutations in 7 out of 17 probands (23.5% of the total IRD cases). In two cases the molecular results allowed a refined clinical diagnosis: a compound heterozygosity of two mutations in *CEP290* led to a genetic diagnosis of LCA in a patient with initial diagnosis of North Carolina or Star-gardt macular dystrophy, whereas a homozygous pathogenic variant in *ABCA4* was found in a patient with tapetoretinal degeneration.

In 36 patients (12 familiar and 24 sporadic) the molecular analysis did not achieve any definitive result, even after the analysis of the healthy family members, which was performed in 8 cases. Half of the cases with a negative test result (18 out of 36) were affected by RP. The additional analysis of the *RPGR* ORF15 (a mutational hotspot which was nonsufficiently covered in our panel) for the male patients with a sporadic or suspected X-linked pattern of inheritance (10 patients) by Sanger sequencing yielded no additional mutations.

4. Discussion

The results of the present study confirm that high-throughput Next-Generation Sequencing represents a comprehensive cost-effective approach for the molecular diagnosis of Inherited Retinal Dystrophies (IRDs), achieving a molecular diagnosis for 59.1% of the studied cases. More specifically, among the different clinical phenotypes, the highest detection rates were achieved for BMD, LCA, USH, and STGD patients, in whom the genetic test clearly confirmed the clinical diagnoses (Table 2). The results of the RP and of the not defined IRD cohorts, instead, demonstrated the high genetic heterogeneity of these diseases and the essential contribution of our NGS analysis to achieving an accurate diagnosis, with the

involvement of 12 different genes in 28 sporadic cases. Revision of the initial diagnosis, performed for 9.6% of the genetically diagnosed patients, further emphasizes the importance of a comprehensive genotype/phenotype analysis to unravel the extensive heterogeneity of these diseases. Notably, a remarkable fraction of identified variants are splice-altering mutations (25% of the total mutation burden, 16 out of 64), located within splicing consensus regions, or exonic variants predicted to cause enhancer/silencer motif modification or the creation of new potential donor/acceptor, which are amenable to the antisense-mediated splicing-correction approaches, as recently reported for several genetic diseases, including *CEP290*-caused LCA [20, 21].

The prevalence of IRD and most importantly the frequency of gene mutations causing those diseases are not well characterized in Italy and only few data have been reported [22–24]. *RPE65*, *CRBI*, and *GUCY2D* were identified as the most prevalent mutated genes in Italian LCA patients [22] and *RHO* was reported to be the gene most commonly responsible for ADRP [23] and *EYS* the most recurrent for nonsyndromic ARRP and sporadic cases [24]. Our study contributes only partially to the knowledge of the gene mutation frequencies, since each IRD type is represented by small cohorts of cases (i.e., the LCA and dominant RP phenotypes were accounted for by 5 and 6 cases, resp.), and some probands of other ethnicities have been included too. Indeed, regarding LCA, we identified mutations in *CEP290*, *RPE65*, *CRX*, and *RPGRIP1* genes.

For ADRP, *RHO* was identified to be responsible for the phenotype in one case, whereas, in ARRP and sporadic RP, *USH2A*, *CNGBI*, and *TULP1* were the most recurrently mutated genes. *RPE65* mutations were found in two ARRP cases: in one more case, still unsolved, a single *RPE65* heterozygous pathogenic variant was found. *ROM1* compound heterozygosity was established in one RP proband, suggesting a mechanism of recessive inheritance for this gene associated with dominant and digenic forms. X-linked inheritance was established for 5 RP affected probands, with *RPGR* and *RP2* identified as the disease-causing gene in 4 cases and 1 case, respectively. All BMD diagnosed patients were heterozygous for mutations on *BEST1* gene, the major gene responsible for Best's juvenile form [25], whereas the 78.5% of patients with clinically diagnosed STGD carried pathogenic variants on *ABCA4* [26].

Similarly to a recent study [6], the clinical sensitivity of our NGS analysis was not uniform, with the highest diagnostic yields obtained in conditions where the disease-causing genes have been nearly all identified.

Direct comparison of our findings with other recently published NGS studies [2–6, 27] is not straightforward, due to differences in the number of genes analyzed but especially due to composition and relative representation of the different phenotypes in the patients cohorts. However, the finding of *USH2A* and *ABCA4* as the most mutated genes for RP/USH and STGD patients is consistent with previous reports [27–29]. In our RP cohort, *USH2A* is followed by *CNGBI* and *RPGR*. These two genes, already reported among the most frequently mutated genes in IRD patients [29], were not highly frequently altered in the Saudi population [6] or

in a large cohort of Western European and South Asian individuals [27]. Also, we did not find any alteration in *EYS*, one of the top three genes contributing to IRD in other populations [28, 29].

The different gene alterations identified in our LCA cohort (*CEP290*, *RPE65*, *RPGRIP1*, and *CRX* genes) were consistent with the different disease manifestations of the analyzed patients, in accordance with the specific clinical features described for each of the LCA-associated genes [30, 31]. Less direct is the correlation between the genes involved and the phenotypic features in RP, due to the known contribution of environmental factors to late-childhood- and adult-onset-diseases.

Allelic heterogeneity, with different mutations in the same gene causing different phenotypes, is evident also in *USH2A*-related retinal disease. Genotype-phenotype correlations observed in our cohort were in accordance with the allelic hierarchy proposed in a recent study [32], supporting the model that USH represents the null phenotype consequent upon severe *USH2A* defects, whereas milder mutations in at least one allele result in a pure retinal phenotype associated with normal auditory function.

IRD genetic heterogeneity, reflected in the identification of mutations in many genes with a considerable number of previously undescribed alterations, supported the conclusion that molecular diagnosis of these disorders should rely on massive parallel multigene sequencing. Nevertheless, for 36 probands, including 12 familiar cases and 24 unrelated probands, our NGS procedure did not result in the identification of a clear genetic cause of the disease. Some subjects may have mutations that cannot be detected by our amplicon-based approach, such as deep intronic mutations, copy-number variations, or large deletions. In the perspective of the design of a more complete new version of the panel, additional deep intronic regions reported in the literature as carrying disease-causing mutations [19, 33, 34] or a higher exon padding (5 bp in our design, up to 100 bp available in the current pipeline version of the Ion AmpliSeq Designer tool) could be implemented. Moreover, technical limitations, including the difficult amplification of *RPGR* ORF15, a mutational hotspot for X-linked RP, may have accounted for some of the missed diagnosis (our panel is presently covering only 30% of this critical exon), but the addition of the specific analysis by Sanger sequencing of the ORF15 of the *RPGR* gene in 10 males patients, with sporadic/X-linked RP and previously testing negative for pathogenic mutations using our NGS panel, did not reveal any mutation in the analyzed region. Finally, as an improvement to further support the pathogenicity of novel mutations identified in probands, the analysis of both affected and unaffected family member should be performed, when possible.

In some of the patients who tested negative we however identified single potentially pathogenic heterozygous mutations in recessive genes or novel heterozygous missense variants in dominant genes with unknown significance, lacking the appropriate level of evidence to classify them as disease-causing or not in concordance with patients' clinical presentations or family data. The contribution of these variants in combination with deep intronic mutations

or large deletions is suspected but could not be demonstrated with the present technique.

Database incompleteness further complicates variant interpretation. Two probands with BMD phenotype and *BEST1* mutation were found to harbour also heterozygous mutation in *RHO* (c.578C>T, p.Thr193Met), which was predicted to be damaging and listed as associated with ADRP in a public database [<http://www.retina-international.org/sci-news/databases/mutation-database>] but in our cohort was carried also by healthy subject, reinforcing the need of a critical interpretation of the molecular findings in view of the phenotypic features of the patients with IRD until a more thorough knowledge of the frequency of the variants and a critical amount of data present in the public disease databases are reached.

In conclusion, by presenting profoundly different mutation rates varying according to the clinical diagnosis and by reporting 9.61% of cases of reassessment of the initial diagnosis on the basis of the results of the test, our study reinforces the need of a multidisciplinary work-up before and after the genetic testing, due to the implications of the results in terms of risk assessment for family members and inclusion in gene-based clinical trials.

Abbreviations/Acronyms

AD:	Autosomal dominant
AR:	Autosomal recessive
BMD:	Best Macular Dystrophy
IRDs:	Inherited Retinal Dystrophies
LCA:	Leber Congenital Amaurosis
NGS:	Next-Generation Sequencing
RP:	Retinitis Pigmentosa
STGD:	Stargardt Disease
USH:	Usher Syndrome
XL:	X-linked.

Competing Interests

No conflicting relationship exists for any author.

Authors' Contributions

Isabella Bernardis and Laura Chiesi contributed equally.

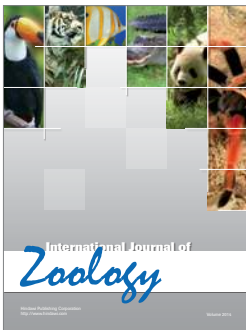
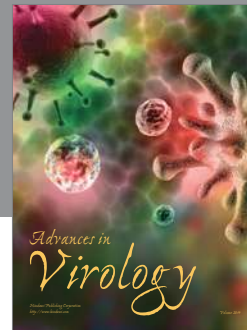
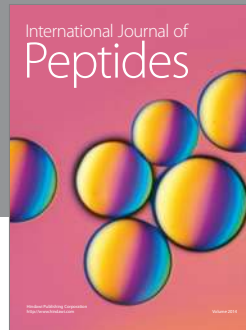
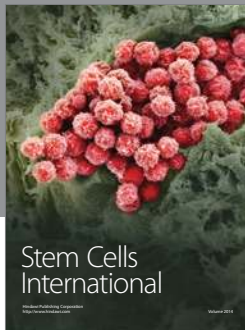
Acknowledgments

This study was supported by Regione Emilia Romagna "RARER," Areal (E35E09000880002). The authors thank Professor Sandro Banfi for kindly providing the control samples used to validate their procedure. Programma di Ricerca Regione-Università 2010–2012 "Next-Generation Sequencing and Gene Therapy to Diagnose and Cure Rare Diseases in Regione Emilia Romagna (RARER)," Area 1, Strategic Programmes (E35E09000880002), is acknowledged. The funding organization participated in the design of the study.

References

- [1] T. P. Dryja, L. B. Hahn, K. Kajiwara, and E. L. Berson, "Dominant and digenic mutations in the peripherin/RDS and ROM1 genes in retinitis pigmentosa," *Investigative Ophthalmology and Visual Science*, vol. 38, no. 10, pp. 1972–1982, 1997.
- [2] K. Neveling, R. W. J. Collin, C. Gilissen et al., "Next-generation genetic testing for retinitis pigmentosa," *Human Mutation*, vol. 33, no. 6, pp. 963–972, 2012.
- [3] T. Eisenberger, C. Neuhaus, A. O. Khan et al., "Increasing the yield in targeted next-generation sequencing by implicating CNV analysis, non-coding exons and the overall variant load: the example of retinal dystrophies," *PLoS ONE*, vol. 8, no. 11, Article ID e78496, 2013.
- [4] J. Wang, V. W. Zhang, Y. Feng et al., "Dependable and efficient clinical utility of target capture-based deep sequencing in molecular diagnosis of retinitis pigmentosa," *Investigative Ophthalmology & Visual Science*, vol. 55, no. 10, pp. 6213–6223, 2014.
- [5] M. B. Consugar, D. Navarro-Gomez, E. M. Place et al., "Panel-based genetic diagnostic testing for inherited eye diseases is highly accurate and reproducible, and more sensitive for variant detection, than exome sequencing," *Genetics in Medicine*, vol. 17, no. 4, pp. 253–261, 2015.
- [6] N. Patel, M. A. Aldahmesh, H. Alkuraya et al., "Expanding the clinical, allelic, and locus heterogeneity of retinal dystrophies," *Genetics in Medicine*, vol. 18, no. 6, pp. 554–556, 2015.
- [7] J. P.-W. Chiang, T. Lamey, T. McLaren, J. A. Thompson, H. Montgomery, and J. De Roach, "Progress and prospects of next-generation sequencing testing for inherited retinal dystrophy," *Expert Review of Molecular Diagnostics*, vol. 15, no. 10, pp. 1269–1275, 2015.
- [8] J. P.-W. Chiang and K. Trzuppek, "The current status of molecular diagnosis of inherited retinal dystrophies," *Current Opinion in Ophthalmology*, vol. 26, no. 5, pp. 346–351, 2015.
- [9] K. Wang, M. Li, and H. Hakonarson, "ANNOVAR: functional annotation of genetic variants from high-throughput sequencing data," *Nucleic Acids Research*, vol. 38, no. 16, article e164, 2010.
- [10] W. McLaren, B. Pritchard, D. Rios, Y. Chen, P. Flicek, and F. Cunningham, "Deriving the consequences of genomic variants with the Ensembl API and SNP Effect Predictor," *Bioinformatics*, vol. 26, no. 16, pp. 2069–2070, 2010.
- [11] X. Liu, X. Jian, and E. Boerwinkle, "dbNSFP: a lightweight database of human nonsynonymous SNPs and their functional predictions," *Human Mutation*, vol. 32, no. 8, pp. 894–899, 2011.
- [12] X. Liu, C. Wu, C. Li, and E. Boerwinkle, "dbNSFP v3.0: a one-stop database of functional predictions and annotations for human nonsynonymous and splice-site SNVs," *Human Mutation*, vol. 37, no. 3, pp. 235–241, 2016.
- [13] C. Dong, P. Wei, X. Jian et al., "Comparison and integration of deleteriousness prediction methods for nonsynonymous SNVs in whole exome sequencing studies," *Human Molecular Genetics*, vol. 24, no. 8, pp. 2125–2137, 2015.
- [14] F.-O. Desmet, D. Hamroun, M. Lalande, G. Collod-Bèroud, M. Claustres, and C. Bèroud, "Human Splicing Finder: an online bioinformatics tool to predict splicing signals," *Nucleic Acids Research*, vol. 37, no. 9, article e67, 2009.
- [15] M. G. Reese, F. H. Eeckman, D. Kulp, and D. Haussler, "Improved splice site detection in Genie," *Journal of Computational Biology*, vol. 4, no. 3, pp. 311–323, 2009.
- [16] X. Jian, E. Boerwinkle, and X. Liu, "In silico prediction of splice-altering single nucleotide variants in the human genome," *Nucleic Acids Research*, vol. 42, no. 22, pp. 13534–13544, 2014.
- [17] H. Y. Xiong, B. Alipanahi, L. J. Lee et al., "The human splicing code reveals new insights into the genetic determinants of disease," *Science*, vol. 347, no. 6218, Article ID 1254806, 2015.
- [18] V. M. Milenkovic, E. Röhrh, B. H. F. Weber, and O. Strauss, "Disease-associated missense mutations in bestrophin-1 affect cellular trafficking and anion conductance," *Journal of Cell Science*, vol. 124, no. 17, pp. 2988–2996, 2011.
- [19] T. A. Braun, R. F. Mullins, A. H. Wagner et al., "Non-exonic and synonymous variants in ABCA4 are an important cause of Stargardt disease," *Human Molecular Genetics*, vol. 22, no. 25, Article ID ddt367, pp. 5136–5145, 2013.
- [20] R. W. Collin, A. I. den Hollander, S. D. van der Velde-Visser, J. Bennicelli, J. Bennett, and F. P. Cremers, "Antisense oligonucleotide (AON)-based therapy for leber congenital amaurosis caused by a frequent mutation in CEP290," *Molecular Therapy Nucleic Acids*, vol. 1, article e14, 2012.
- [21] N. Bacchi, S. Casarosa, and M. A. Denti, "Splicing-correcting therapeutic approaches for retinal dystrophies: where endogenous gene regulation and specificity matter," *Investigative Ophthalmology and Visual Science*, vol. 55, no. 5, pp. 3285–3294, 2014.
- [22] F. Simonelli, C. Ziviello, F. Testa et al., "Clinical and molecular genetics of Leber's congenital amaurosis: a multicenter study of Italian patients," *Investigative Ophthalmology & Visual Science*, vol. 48, no. 9, pp. 4284–4290, 2007.
- [23] C. Ziviello, F. Simonelli, F. Testa et al., "Molecular genetics of autosomal dominant retinitis pigmentosa (ADRP): a comprehensive study of 43 Italian families," *Journal of Medical Genetics*, vol. 42, no. 7, p. e47, 2005.
- [24] C. O. Pierrotet, M. Zuntini, M. Digiuni et al., "Syndromic and non-syndromic forms of retinitis pigmentosa: a comprehensive Italian clinical and molecular study reveals new mutations," *Genetics and Molecular Research*, vol. 13, no. 4, pp. 8815–8833, 2014.
- [25] F. Krämer, K. White, D. Pauleikhoff et al., "Mutations in the VMD2 gene are associated with juvenile-onset vitelliform macular dystrophy (Best disease) and adult vitelliform macular dystrophy but not age-related macular degeneration," *European Journal of Human Genetics*, vol. 8, no. 4, pp. 286–292, 2000.
- [26] V. C. Sheffield and E. M. Stone, "Genomics and the eye," *The New England Journal of Medicine*, vol. 364, no. 20, pp. 1932–1942, 2011.
- [27] J. M. Ellingford, S. Barton, S. Bhaskar et al., "Molecular findings from 537 individuals with inherited retinal disease," *Journal of Medical Genetics*, vol. 53, no. 11, pp. 761–767, 2016.
- [28] X.-F. Huang, F. Huang, K.-C. Wu et al., "Genotype-phenotype correlation and mutation spectrum in a large cohort of patients with inherited retinal dystrophy revealed by next-generation sequencing," *Genetics in Medicine*, vol. 17, no. 4, pp. 271–278, 2015.
- [29] Z. Ge, K. Bowles, K. Goetz et al., "NGS-based Molecular diagnosis of 105 eyeGENE(®) probands with Retinitis Pigmentosa," *Scientific Reports*, vol. 5, p. 18287, 2015.
- [30] S. Hanein, I. Perrault, S. Gerber et al., "Leber congenital amaurosis: comprehensive survey of the genetic heterogeneity, refinement of the clinical definition, and genotype-phenotype correlations as a strategy for molecular diagnosis," *Human Mutation*, vol. 23, no. 4, pp. 306–317, 2004.

- [31] F. Coppieters, I. Casteels, F. Meire et al., “Genetic screening of LCA in Belgium: predominance of CEP290 and identification of potential modifier alleles in AHI1 of CEP290-related phenotypes,” *Human Mutation*, vol. 31, no. 10, pp. E1709–E1766, 2010.
- [32] E. Lenassi, A. Vincent, Z. Li et al., “A detailed clinical and molecular survey of subjects with nonsyndromic USH2A retinopathy reveals an allelic hierarchy of disease-causing variants,” *European Journal of Human Genetics*, vol. 23, no. 10, pp. 1318–1327, 2015.
- [33] A. Liquori, C. Vaché, D. Baux et al., “Whole USH2A gene sequencing identifies several new deep intronic mutations,” *Human Mutation*, vol. 37, no. 2, pp. 184–193, 2016.
- [34] A. I. den Hollander, R. K. Koenekoop, S. Yzer et al., “Mutations in the CEP290 (NPHP6) gene are a frequent cause of Leber congenital amaurosis,” *The American Journal of Human Genetics*, vol. 79, no. 3, pp. 556–561, 2006.



Hindawi

Submit your manuscripts at
<http://www.hindawi.com>

